Use of the Transmission-Line Super Theory to Determine Generalized Reflection and Transmission Coefficients of an Inhomogeneous Line with Risers

Sergey Tkachenko*, Ronald Rambousky**, and Jürgen Nitsch*

* Otto-von-Guericke University Magdeburg, Germany
** Bundeswehr Research Institute for Protective Technologies and NBC Protection (WIS), Munster, Germany

Abstract

The analysis conducted within the framework of Transmission-Line Super Theory (TLST) has led to new formulations for the reflection and transmission coefficients of inhomogeneous transmission lines at high frequencies. In this paper, these results are derived and applied for the first time on practical non-uniform conductor configurations. The results obtained agree excellently with the exact TLST solutions, although the new expressions contain a certain approximation: the radiation phenomena are only considered within the individual inhomogeneous parts of the lines.

Content

I. INTRODUCTION

In a number of applications in electrical engineering and electronics it is necessary to calculate currents and voltages propagating in wiring structures, like, e.g., antennas and transmission lines. A well-known, convenient tool for such calculations is the classical transmission line approximation (TL). Classical TL leads to explicit analytical expressions and allows one to carry out qualitative analysis and engineering calculations for such systems, practically instantaneously. However, the TL is valid only up to frequencies for which the wavelength is comparable with the transversal dimension of the line. In modern electronics, however, the working range of the signal frequencies is continually to increasing. Moreover, the wiring structures can work as a receiver of intentional and unintentional interferences of different kind, and at the same time, the sensitivity of the modern semiconductor elements is also increasing. All these circumstances require the development of corresponding calculation methods. The pure numerical methods, like MoM, TLT, etc., have long calculation times; they also can only consider the specific case and don't allow investigating the problem in general. The alternatives are different analytical and analytical – numerical methods.

One of the most promising methods is the Transmission Line Super Theory, TLST, [1-8] which reduces the system of exact integro-differential equations (Mixed Potential Integral Equations – MPIE) to a system of the first order ordinary differential equations. This system looks like the system of inhomogeneous Telegrapher's equations, but with complex-valued parameters and non-zero diagonal elements (see Section 2). The parameters of the system can be obtained using an iteration procedure, which, in turn, requires quite long calculations.

However, in reality, the lines consist of some non-uniform regions (near terminal regions, different bends, lumped sources and/or loads, etc.), which are connected with each other by regions having a uniform structure of classical TL (wire is parallel to conducting ground). The solution for the current near the non-uniformities has a complex structure including different type of modes: leaky modes, radiation modes and TEM modes. Usually, the non-uniform regions are essentially shorter than the uniform regions. This means that the current in the long, central region(s) can be solved for in a simple manner. Their solutions look like solutions of inhomogeneous exact integro – differential equations for the infinitely long line (for the case of excitation by an external field) plus two solutions of homogeneous integro – differential equations for the infinite transmission line (forward and backward propagating TEM modes). The coefficients for the TEM modes are defined by the so called reflection (transmission) and amplitude coefficients for current waves [9, 10, 17]. Such a solution for the induced current (the so-called asymptotical solution) formally looks like a solution in TL approximation, but with other values of reflection and transmission coefficients[1]. Of course, for low frequencies, when one can use simple formulas for these coefficients, the asymptotic solution becomes a solution of the classical theory of transmission lines.

To obtain these coefficients one can use an iteration method for the semi – infinite line (see [10], [12], [13]) with the same (left or right) terminal, but it requires some analytical calculations. Another method is a processing result of the TLST for shorter lines. It allows the developed methods and software of TLST to be used. Moreover, it installs a deep physical connection between the asymptotic method, TLST and SEM [13, 18]. The aim of the present research is to obtain the reflection (transmission) and amplitude coefficients for current waves using the method of Transmission Line Super Theory. General formulas are obtained which

---

[1] Such representation is convenient for the analysis of the Singularity Expansion Method (SEM) of the poles in the first layer for such a transmission line system (see, e.g., [11]). Knowledge of these poles, in turn, allows one to obtain analytical results for the response in the time domain.

are then checked by calculating the simple, but not trivial examples of a straight and a bent horizontal line with risers.

II. ESSENTIALS OF THE TLST AND STATEMENT OF THE PROBLEM

1. Definition of the global parameters of TLST

Consider a thin wire of arbitrary geometric form, $\vec{r}(l)$ (where l is the coordinate along the wire axis) above a perfectly conducting ground (see, for example, the non-uniform wire with vertical elements in Fig.1) which may be loaded and excited by an external field $\vec{E}^{i}(\vec{r})$.
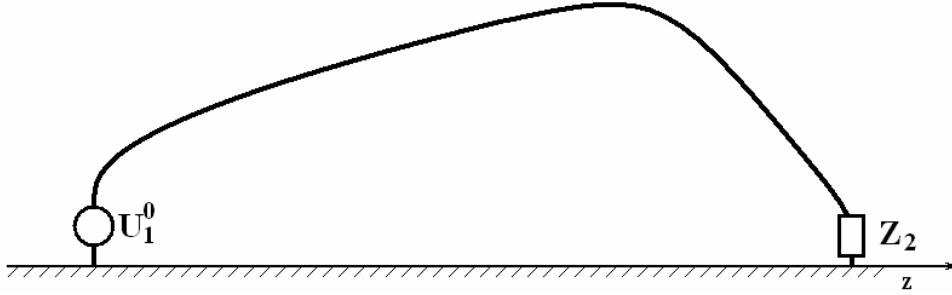

Fig. 1: Geometry of the transmission line structure.

Using the zero boundary conditions for the total (scattering plus exciting) tangential electric field on the surface of the wire and the continuity equation for the induced current, we obtain a system of integro-differential equations for the "current and potential" pair (Mixed Potential Integral Equations – MPIE):

$$\begin{cases} \dfrac{d\,\varphi(l)}{d\,l} + j\omega\dfrac{\mu_0}{4\pi}\int_0^L g_I^L(l,l')\,I(l')\,dl' = E_l^e(l) \\[3mm] \int_0^L g_I^C(l,l')\dfrac{d\,I(l')}{d\,l'}dl' + j\omega\,4\pi\varepsilon_0\,\varphi(l) = 0 \end{cases}$$

(1 a, b)

Here $E_l^e(l)$ is an exciting total tangential electric field (incident plus reflected), $\varphi(l)$ is the scalar potential along the wire (in the Lorenz gauge), a the radius of the wire, and L is the total length of the wire. The functions $g_I^L(l,l')$ and $g_I^C(l,l')$ are the Green's functions along the curved line for the vector potential and scalar potential, respectively, which take into account the reflection of the ground plane:

$$g_I^C(l,l') = \frac{e^{-jk\sqrt{(\vec{r}(l)-\vec{r}(l'))^2+a^2}}}{\sqrt{(\vec{r}(l)-\vec{r}(l'))^2+a^2}} - \frac{e^{-jk\sqrt{(\vec{r}(l)-\tilde{\vec{r}}(l'))^2+a^2}}}{\sqrt{(\vec{r}(l)-\tilde{\vec{r}}(l'))^2+a^2}}$$

(2)

$$g_I^L(l,l') = \vec{e}_l(l)\cdot\vec{e}_l(l')\frac{e^{-jk\sqrt{(\vec{r}(l)-\vec{r}(l'))^2+a^2}}}{\sqrt{(\vec{r}(l)-\vec{r}(l'))^2+a^2}} - \vec{e}_l(l)\cdot\tilde{\vec{e}}_l(l')\frac{e^{-jk\sqrt{(\vec{r}(l)-\tilde{\vec{r}}(l'))^2+a^2}}}{\sqrt{(\vec{r}(l)-\tilde{\vec{r}}(l'))^2+a^2}}$$

(3)

The unit tangential vector $\vec{e}_l(l) = d\vec{r}(l)/dl$ of the curve is taken along the wire axis, $\vec{\tilde{r}}(l)$ is the radius vector reflected by the ground plane, and $\vec{\tilde{e}}_l(l) = d\vec{\tilde{r}}(l)/dl$ is the corresponding unit tangential vector.

Now, in order to define the global generalized transmission line parameters, consider an excitation of the transmission line by a lumped voltage source U_1^0 located at the beginning of the line. The line is also assumed to be loaded by a lumped impedance Z_2 at the far end. There are two possibilities to account for the source and the load: either to treat both of them as boundary conditions or treat both of them as sources (with unknown amplitude for the "load source"). For the second possibility the exciting field $E_l^e(l)$ can be written as [5]:

$$E^e{}_l(l) = U_1 \delta(l - \Delta) + U_2 \delta(l - L + \Delta) \tag{4}$$

$$U_2 = -Z_2 I(L - \Delta) \qquad \text{with } \Delta \to 0 \tag{5}$$

Of course, in the formal view (4) one can also represent a problem with excitations at two terminals, with excitation at the right terminal and loading at left terminal, etc.

The admittance functions $Y_1(l), Y_2(l)$ have dimensions of conductance while the transfer functions for the potential $K_1(l), K_2(l)$ are dimensionless. Now let the response functions $Y_1(l)$, $Y_2(l)$ and $K_1(l)$, $K_2(l)$ be solutions of the system (1 a,b) for the current and the potential with sources of amplitude 1 V $\delta(l - \Delta)$, $\delta(l - L + \Delta)$ located in the points Δ and $L - \Delta$, respectively. Due to the linearity of the considered problem we can write the solution for the total induced current as

$$I(l) = U_1^0 Y_1(l) + U_2^0 Y_2(l) \tag{6}$$

For the potential $\varphi(l)$ along the wire one finds a similar equation:

$$\varphi(l) = U_1^0 K_1(l) + U_2^0 K_2(l) \tag{7}$$

Now one is ready to look for the system of differential equations for the potential and current in TL-like form:

$$\frac{d\varphi(l)}{dl} + j\omega P_{12}(l) I(l) + j\omega P_{11}(l) \varphi(l) = 0$$

$$\frac{dI(l)}{dl} + j\omega P_{21}(l) \varphi(l) + j\omega P_{22}(l) I(l) = 0 \tag{8a, b}$$

Because the values U_1^0 and U_2^0 are linearly independent, the equations (8) have to be satisfied for each column $(Y_1(l), K_1(l))^T$ and $(Y_2(l), K_2(l))^T$ (in matrix form):

$$\frac{d}{dl}\begin{pmatrix} Y_1(l) & Y_2(l) \\ K_1(l) & K_2(l) \end{pmatrix} = j\omega \begin{pmatrix} P_{11}(l) & P_{12}(l) \\ P_{21}(l) & P_{22}(l) \end{pmatrix} \cdot \begin{pmatrix} Y_1(l) & Y_2(l) \\ K_1(l) & K_2(l) \end{pmatrix} \tag{9}$$

Using equation (9) one can evaluate the equation for the parameter matrix $\hat{P}(l)$:

$$\hat{P}(l) = -\frac{1}{j\omega} \frac{d}{dl}\begin{pmatrix} Y_1(l) & Y_2(l) \\ K_1(l) & K_2(l) \end{pmatrix} \cdot \begin{pmatrix} Y_1(l) & Y_2(l) \\ K_1(l) & K_2(l) \end{pmatrix}^{-1} \tag{10}$$

It is easy to show that the choice of "basic" solutions does not influence the value of the parameters. In fact, considering a new system of basic functions as a non-degenerate linear combination of the previous one results in:

$$\begin{pmatrix} \widetilde{Y}_1(l) & \widetilde{Y}_2(l) \\ \widetilde{K}_1(l) & \widetilde{K}_2(l) \end{pmatrix} := \begin{pmatrix} Y_1(l) & Y_2(l) \\ K_1(l) & K_2(l) \end{pmatrix} \cdot \begin{pmatrix} \alpha_{11} & \alpha_{12} \\ \alpha_{21} & \alpha_{22} \end{pmatrix} =$$

$$= \begin{pmatrix} Y_1(l)\alpha_{11} + Y_2(l)\alpha_{21} & Y_1(l)\alpha_{12} + Y_2(l)\alpha_{22} \\ K_1(l)\alpha_{11} + K_2(l)\alpha_{21} & K_1(l)\alpha_{12} + K_2(l)\alpha_{22} \end{pmatrix}$$

$$\det(\hat{\alpha}) \neq 0 \qquad (11)$$

Then, calculating the parameters we have:

$$\hat{\widetilde{P}}(l) = -\frac{1}{j\omega}\frac{d}{dl}\begin{pmatrix} \widetilde{Y}_1(l) & \widetilde{Y}_2(l) \\ \widetilde{K}_1(l) & \widetilde{K}_2(l) \end{pmatrix} \cdot \begin{pmatrix} \widetilde{Y}_1(l) & \widetilde{Y}_2(l) \\ \widetilde{K}_1(l) & \widetilde{K}_2(l) \end{pmatrix}^{-1} =$$

$$-\frac{1}{j\omega}\left[\frac{d}{dl}\begin{pmatrix} Y_1(l) & Y_2(l) \\ K_1(l) & K_2(l) \end{pmatrix} \cdot \begin{pmatrix} \alpha_{11} & \alpha_{12} \\ \alpha_{21} & \alpha_{22} \end{pmatrix}\right] \cdot \left[\begin{pmatrix} Y_1(l) & Y_2(l) \\ K_1(l) & K_2(l) \end{pmatrix} \cdot \begin{pmatrix} \alpha_{11} & \alpha_{12} \\ \alpha_{21} & \alpha_{22} \end{pmatrix}\right]^{-1} = \qquad (11a)$$

$$= -\frac{1}{j\omega}\frac{d}{dl}\begin{pmatrix} Y_1(l) & Y_2(l) \\ K_1(l) & K_2(l) \end{pmatrix} \cdot \begin{pmatrix} Y_1(l) & Y_2(l) \\ K_1(l) & K_2(l) \end{pmatrix}^{-1} = \hat{P}(l)$$

Thus, it is shown that the system of integro-differential equations (1), with a solution which is defined by two independent constants, can be explicitly reduced to the differential equations (8) with parameters (9). These parameters are either global parameters in the full-wave transmission line theory or the parameters of "Maxwellian circuits", and they are complex valued. Moreover, they also describe the radiation of the system [4, 5, 6]. They depend on the geometry of the system, and, therefore, on the local geometric parameter l along the line. This fact was already established in [1, 2, 3, 6] with the method of the product integral, and in [14] by processing the numerical solutions for the current and potential with the Method of Moments.

The parameter matrix $\hat{P}(l)$ depends on the gauge of the potential φ. For example, it has a different form for the Coulomb gauge than it has for the Lorenz gauge.

2. Matrizant and its application for solution of TLST equations.

As mentioned in the previous sub-section, the parameter matrix can be defined on any pair of linear independent solutions of the integro – differential MPIE system (a homogeneous system), and this system is also a solution of the corresponding ODE system with parameter matrix $\hat{P}(l)$ and some boundary conditions (which have not yet been defined). Further, it is convenient to consider the matrix of solutions, which satisfy the following boundary conditions:

$$\hat{M}_0^l(-j\omega\hat{P}) := \begin{pmatrix} \varphi_1(l) & \varphi_2(l) \\ I_1(l) & I_2(l) \end{pmatrix}; \qquad \begin{pmatrix} \varphi_1(0) & \varphi_2(0) \\ I_1(0) & I_2(0) \end{pmatrix} = \begin{pmatrix} 1 & 0 \\ 0 & 1 \end{pmatrix} \qquad (12a, b)$$

Due to the linearity of the problem, if we have arbitrary boundary conditions $(\varphi(0), I(0))^T$, the solution for the coordinate l looks like:

$$\begin{pmatrix} \varphi(l) \\ I(l) \end{pmatrix} = \hat{M}_0^l(-j\omega\hat{P}) \cdot \begin{pmatrix} \varphi(0) \\ I(0) \end{pmatrix} \qquad (13)$$

The matrix $\hat{M}_0^l(-j\omega\hat{P})$ is called the matrizant, product integral or propagator [15]. It "translates" the solution from the point $l = 0$ to the point l. More generally written:

$$\begin{pmatrix} \varphi(l) \\ I(l) \end{pmatrix} = \hat{M}_{l_0}^l(-j\omega\hat{P}) \cdot \begin{pmatrix} \varphi(l_0) \\ I(l_0) \end{pmatrix} \qquad (14)$$

The matrizant can be easily calculated by the division of the interval (l_0, l) into small (limited, infinitesimal) subintervals Δl_i ($N \to \infty$) and the calculation of the matrix product (product integral)^2 is as follows:

$$\hat{M}_{l_0}^l(-j\omega\hat{P}) = \lim_{\Delta l_i \to 0} \prod_{i=1}^{N} \left(\hat{I} - j\omega\hat{P}(l_i)\Delta l_i \right) = \lim_{\Delta l_i \to 0} \prod_{i=1}^{N} \exp(-j\omega\hat{P}(l_i)\Delta l_i) \qquad (15)$$

For the homogeneous parameter line, when the parameter matrix is constant, the matrizant is just a matrix exponent:

$$\hat{M}_{l_0}^l(-j\omega\hat{P}_0) = \exp(-j\omega\hat{P}_0(l - l_0)) \qquad (16)$$

Once the matrizant is known, it becomes possible to find a solution with the given boundary problems. For example, for the simple boundary problem, described in Fig. 1, one has for any point l :

$$\begin{pmatrix} \varphi(l) \\ I(l) \end{pmatrix} = \hat{M}_0^l(-j\omega\hat{P}) \cdot \begin{pmatrix} U_0 \\ I(0) \end{pmatrix} \qquad (17)$$

But, here the current in the point $l = 0$ is unknown. To find it one uses the second boundary condition:

$$\begin{pmatrix} \varphi(L-\Delta) \\ I(L) \end{pmatrix} = \begin{pmatrix} Z_2 I(L) \\ I(L) \end{pmatrix} = \hat{M}_0^l(-j\omega\hat{P}) \cdot \begin{pmatrix} U_0 \\ I(0) \end{pmatrix} \qquad (18)$$

This yields two equations for the unknown currents:

$$I(0) = U_0 \frac{Z_2 M_0^L(-j\omega\hat{P})_{21} - M_0^L(-j\omega\hat{P})_{11}}{M_0^L(-j\omega\hat{P})_{12} - Z_2 M_0^L(-j\omega\hat{P})_{22}}$$

$$I(L) = -U_0 \frac{M_0^L(-j\omega\hat{P})_{11} M_0^L(-j\omega\hat{P})_{22} - M_0^L(-j\omega\hat{P})_{12} M_0^L(-j\omega\hat{P})_{21}}{M_0^L(-j\omega\hat{P})_{12} - Z_2 M_0^L(-j\omega\hat{P})_{22}} \qquad (19a, b)$$

---

^{2} Another way to calculate the matrizant is to use an infinite series of perturbation theory – Volterra series. This and many another properties of matrizant are described in [15].

Eq. (13) with (19a) yields the solution in an arbitrary point l.

3. *Approximate equations for the global parameters of TLST (perturbation theory).*

The solution of system (8a, b) with parameter matrix $[P(l)]$ of (10) and usual boundary conditions for the currents and voltages (differences of potentials) in the points $l = \Delta$ and $l = L - \Delta$ (obtained by the matrizant method described in the previous subsection or by any other method) yields the current and voltage distribution along the line for arbitrarily given values of the terminal sources and loads. The procedure is convenient, when the exact values of the functions $Y_1(l), Y_2(l)$ and $K_1(l), K_2(l)$ are known, from either known analytical solutions [4, 5] or numerical solutions [15]. Another way is to organize some iteration procedure. Generally, the approximate solution of the system (1) is defined in the first step. Then this solution is used to find the corresponding parameters, etc. In [1-3] and [7, 8] the static distributions for the current and potential were used as the lowest iteration step. The first iteration for the parameters was obtained after some numerical procedures.

Another procedure, which is based on the assumption of a thin wire, is proposed in [4, 5, 16]. In the zeroth step in this procedure the system (1) (within the logarithmical accuracy) was reduced to a classical TL system with constant parameters. The solution of this system with its sources (4) yields the functions for the current of the first iteration, $Y_1(l)$ and $Y_2(l)$, of which the linear combinations can be represented up to a constant factor as forward and backward propagating current waves:

$$I_1^{(1)}(l) = e^{-jkl} \qquad\qquad I_2^{(1)}(l) = e^{jkl} \qquad\qquad (21\ a, b)$$

However, exact equations (1a, b) are used for the scalar potential in the first iteration and for its derivative. After straightforward calculations one obtains the parameter matrix in the first order approximation:

$$\hat{P}^{(1)}(l) = \frac{1}{\dfrac{1}{C_+'^{(1)}(l)} + \dfrac{1}{C_-'^{(1)}(l)}} \begin{pmatrix} c\left(L_+'^{(1)}(l) - L_-'^{(1)}(l)\right) & \dfrac{L_+'^{(1)}(l)}{C_-'^{(1)}(l)} + \dfrac{L_-'^{(1)}(l)}{C_+'^{(1)}(l)} \\ 2 & -\dfrac{1}{c}\left(\dfrac{1}{C_+'^{(1)}(l)} - \dfrac{1}{C_-'^{(1)}(l)}\right) \end{pmatrix} \qquad (22)$$

In Eq. (22) one has used the following expressions for the approximate "inductance" and "capacitance", respectively:

$$L_\pm'^{(1)}(l) = \frac{\mu_0}{4\pi} \cdot \int_0^L g_I^L(l,l') e^{\mp jk(l'-l)}\, dl' \ ; \qquad C_\pm'^{(1)}(l) = \frac{4\pi\varepsilon_0}{\displaystyle\int_0^L g_I^C(l,l') e^{\mp jk(l'-l)}\, dl'} \qquad (23a, b)$$

Further, as mentioned in the Introduction, assuming that the matrix of parameters is known, one defines the reflection and transmission coefficients using the components of the matrizant. In the next section, it will be shown how this knowledge can be used to calculate the response of a long line with relatively small non-uniform pieces.

III. DETERMINATION OF THE REFLECTION- AND TRANSMISSION-COEFFICIENTS

1. Classical transmission-line theory

From classical transmission-line theory for a thin and lossless wire above perfectly conducting ground one knows the corresponding physical equations for voltage and current

$$\frac{dU(z)}{dz} + j\omega L'I(z) = 0 \quad \text{and} \quad \frac{dI(z)}{dz} + j\omega C'U(z) = 0, \quad \mapsto \quad U(z) = -\frac{1}{j\omega C'}\frac{dI}{dz} \quad (24\text{a,b,c})$$

From these equations one can derive forward and backward running voltage or current waves and, with their aid, define the reflection coefficients at both ends of a terminated line. In the following section and throughout the rest of the paper, the use of current waves is preferred. First, the reflection coefficient at the beginning of the line shall be determined. For this purpose it is assumed that an incoming wave comes from the right, is reflected at the beginning of the line and runs back to the right hand side of the line which is terminated by its characteristic impedance. This avoids reflections from the end of the line. Expressed in formulae, the current and voltage then read (using (24b, c) :

$$I(z) = I_1\left(\underbrace{e^{jkz}}_{incoming\ wave} + \underbrace{R_+e^{-jkz}}_{outgoing\ wave}\right) \quad \text{and} \quad U(z) = I_1 Z_C\left(-e^{jkz} + R_+e^{-jkz}\right) \quad (25,\text{a,b})$$

Equations 25 a and b are now solved with respect to R_+ and result in:

$$R_+ = e^{2jkz}\frac{U(z) + Z_C I(z)}{-U(z) + Z_C I(z)} \quad (26)$$

Inserting the known solutions of classical transmission-line theory for $U(z)$ and $I(z)$, whereby the matrizant elements are sine and cosine functions, results in

$$M(z,0) = \begin{pmatrix} \cos(kz) & -jZ_C\sin(kz) \\ -\dfrac{j}{Z_C}\sin(kz) & \cos(kz) \end{pmatrix} \quad (27\text{a})$$

$$\text{and} \quad \begin{pmatrix} U(z) \\ I(z) \end{pmatrix} = \begin{pmatrix} \cos(kz) & -jZ_C\sin(kz) \\ -\dfrac{j}{Z_C}\sin(kz) & \cos(kz) \end{pmatrix}\begin{pmatrix} U(0) \\ I(0) \end{pmatrix} = I(0)M(z,0)\begin{pmatrix} -Z_0 \\ 1 \end{pmatrix} \quad (27\text{b})$$

one obtains for $\forall z \in [0, L_{TL}]$ the constant reflection coefficient:

$$R_+ = \frac{Z_C - Z_0}{Z_C + Z_0} \quad (28)$$

In order to obtain the right hand side reflection coefficient R_- one has instead of (25a):

$$I(z) = I_2\left(\underbrace{e^{-jk(z-L_{TL})}}_{incoming\ wave} + \underbrace{R_-e^{jk(z-L_{TL})}}_{outgoing\ wave}\right) \quad (29)$$

and instead of (26) one gets:

$$R_- = e^{-2jk(z-L_{TL})} \frac{-U(z)+Z_C I(z)}{U(z)+Z_C I(z)} \tag{30}$$

Now, again using the proper matrizant expression for $U(z)$ and $I(z)$ in (30)

$$\begin{pmatrix} U(z) \\ I(z) \end{pmatrix} = M(z,L_{TL}) \begin{pmatrix} U(L_{TL}) \\ I(L_{TL}) \end{pmatrix} = I(L_{TL}) M(z,L_{TL}) \begin{pmatrix} Z_{L_{TL}} \\ 1 \end{pmatrix} \tag{31}$$

and arrives at the known result:

$$R_- = \frac{Z_C - Z_L}{Z_C + Z_L} \tag{32}$$

Eventually, it is also known from classical transmission-line theory that the current along the line can be expressed with the aid of the reflection coefficients as

$$I(z) = U_0 \cdot \frac{1}{Z_0 + Z_C} \cdot \frac{1}{1 - R_+ R_- e^{-2jkL_{TL}}} \cdot \left(e^{-jkz} + R_- \cdot e^{-jk(2L_{TL}-z)} \right) \tag{33}$$

Here, the quantity L_{TL} denotes the (horizontal) length of the line. The risers are not taken into account in cTLT due to the condition kh<<1.
The term in (33)

$$\left(U_0 / (Z_0 + Z_C) \right) e^{-jkz}$$

denotes the first outgoing current wave before it is reflected for the first time at the end. Thus it can be written as

$$I(z) =: C_+(z) e^{-jkz} = \underbrace{\frac{U(z)+Z_C I(z)}{2Z_C}}_{\text{forward running wave}} = \left(U_0 / (Z_0 + Z_C) \right) e^{-jkz} \tag{33a}$$

The numerator of the middle quotient in (33a) is a forward running current wave which is normalized with $2Z_C$. The function $C_+(z)$ can be expressed by:

$$C_+(z) = e^{jkz} \frac{U(z)+Z_C I(z)}{2Z_C} \quad , \tag{33b}$$

an expression that one will encounter again later on.
At this point the question arises whether the above results of classical TL theory can be applied in a generalized form in TLST, and if so, under which restrictions.

2. The Reflection Coefficients at the ends of the line in TLST

The first observation in a description of a classical transmission-line configuration in the framework of TLST is the inclusion of the risers at both ends of the line. Moreover, as a Maxwellian theory, in the TLST the line parameters become complex valued, depend on frequency and local coordinates, and the conductor radiates. Obviously, most of the radiation of electromagnetic energy is emitted around the bends connecting the horizontal part of the line with the risers. Since, however, radiation is a long-ranging interaction every part of the line is principally affected. Nevertheless, there is an extended part of the horizontal piece of the line, in which the radiation can be neglected and the TEM mode dominates. All other modes mainly occur around the bends. Thus, along the TEM mode sections of the line the potential represents voltage and can be measured.

10

For the following analysis it is assumed that along the considered non-homogeneous line sections exist that are dominated by TEM modes which separate those parts of the conductor which are non-homogeneous. De facto, this means that such non-uniform line parts which are separated by uniform line pieces do not interact by radiation. For a classical line configuration it follows that the radiation interaction between the two risers is neglected. To fulfill this requirement, the length of the line must be much larger than its height.

In the TLST the voltage $U(z)$ of cTLT is replaced by the potential $\varphi(l)$ and the current $I(z)$ by $i(l)$. The parameter l denotes the natural parameter (arc length) along the line. The solutions for the potential and the current are assumed to be known by the matrizant. Then in analogy to the above considerations the generalized reflection coefficients are defined by the quotients of incoming and outgoing current waves:

$$\tilde{R}_-(l) := e^{-2jk(l-L)} \frac{i(l)Z_C - \varphi(l)}{i(l)Z_C + \varphi(l)} \quad \text{and} \quad \tilde{R}_+(l) := e^{2jkl} \frac{\varphi(l) + Z_C i(l)}{-\varphi(l) + Z_C i(l)} \tag{34a,b}$$

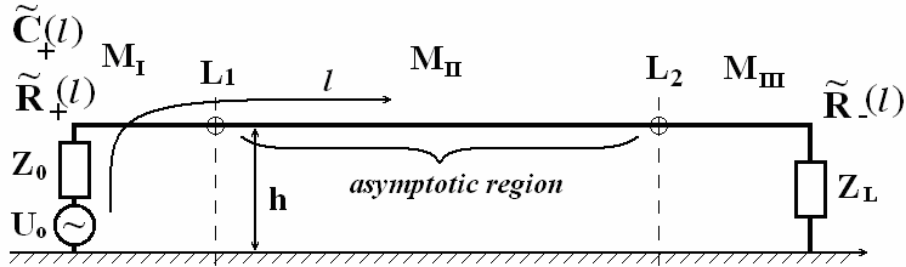The investigated conductor configuration is depicted in Figure 2.

Fig.2: Schematic line configuration. L denotes the total length, L_1 is the coordinate where the TEM region begins and L_2 where the TEM region ends. U_0 is the feeding source, Z_0 and Z_L are the terminations, h is the height of the line above ground.

As can be seen from Fig.2 the conductor is divided into three parts: Two inhomogeneous parts which run from $l = 0$ to $l = L_1$ and from $l = L_2$ to $l = L$. The third part of the line concerns the central TEM region, in which the classical solutions apply.

As assumed the solution for the total line is given by the matrizant $M(L, 0)$. Due to the group property of the matrizant the total solution can be broken down into partial solutions for certain sections of the line. For the case shown in Fig.2 one can write:

$$M(L, 0) = M_{III}(L, L_2) \cdot M_{II}(L_2, L_1) \cdot M_I(L_1, 0) \tag{35}$$

Here $M_{II}(L_2, L_1)$ coincides with the solution in (27a). At the connection points L_1 and L_2, the line parameters have to be adjusted accordingly, so that the product solution gives the total solution (see Ref. [17]).

3. Calculation of the reflection coefficient at the end of the line

To calculate $\tilde{R}_-(l)$ consider a current wave coming from minus infinity and running to the right end of the conductor. There it is reflected by $\tilde{R}_-(l)$ and runs back to infinity. An incoming wave from infinity was chosen to receive no reflections from the left end of the line.

11

This can also be achieved by terminating the line on the left side with the characteristic impedance (see Figure 3).
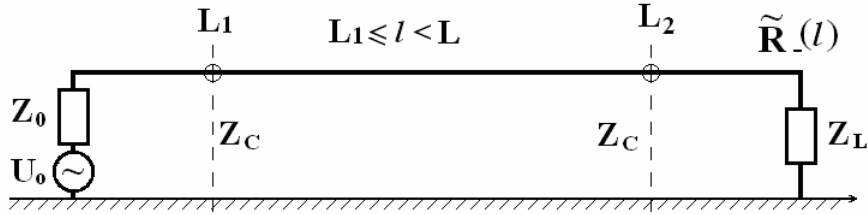

Fig.3: For the calculation of $\tilde{R}_-(l)$.

The quotient in (34a) is now expressed by the elements of the matrizant. Taking into account the boundary condition at the right hand side of the wire $\varphi(L) = U_L = Z_L i(L)$ one gets via the matrizant relation

$$\begin{pmatrix} \varphi(l) \\ i(l) \end{pmatrix} = M(l,L) \begin{pmatrix} \varphi(L) \\ i(L) \end{pmatrix} = i(L) M(l,L) \begin{pmatrix} Z_L \\ 1 \end{pmatrix} \quad , \quad L_1 < l \le L \tag{36}$$

the desired final result for $\tilde{R}_-(l)$:

$$\tilde{R}_-(l) = e^{-2jk(l-L)} \frac{M_{21}(l,L) Z_L Z_C - M_{12}(l,L) + M_{22}(l,L) Z_C - M_{11}(l,L) Z_L}{M_{21}(l,L) Z_L Z_C + M_{12}(l,L) + M_{22}(l,L) Z_C + M_{11}(l,L) Z_L} \tag{37}$$

In a similar manner, $\tilde{R}_+(l)$ will be determined next.

4. The Reflection coefficient at the beginning of the line

In this case, it is assumed that a current wave coming from the right is reflected at the beginning of the line by $\tilde{R}_+(l)$. This situation is illustrated in Figure 4.
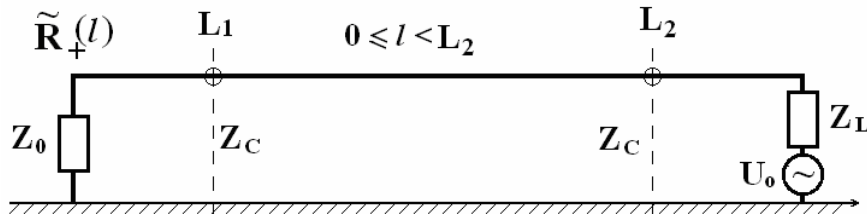

Fig.4: Conductor configuration to calculate $\tilde{R}_+(l)$.

Now the quotient (34b) is expressed by the matrizant elements taking into account the boundary condition at the left side of the conductor: $\varphi(0) = -Z_0 i(0)$. One has:

$$\begin{pmatrix} \varphi(l) \\ i(l) \end{pmatrix} = M(l,0) \begin{pmatrix} \varphi(0) \\ i(0) \end{pmatrix} = i(0) M(l,0) \begin{pmatrix} -Z_0 \\ 1 \end{pmatrix}, \quad 0 \le l < L_2 \tag{38}$$

Then, insertion of $\varphi(l)$ and $i(l)$ from (38) into (34b) yields the following for $\tilde{R}_+(l)$:

$$\tilde{R}_+(l) = e^{2jkl} \frac{-M_{21}(l,0) Z_0 Z_C + M_{12}(l,0) - M_{11}(l,0) Z_0 + M_{22}(l,0) Z_C}{-M_{21}(l,0) Z_0 Z_C - M_{12}(l,0) + M_{11}(l,0) Z_0 + M_{22}(l,0) Z_C} \tag{39}$$

5. The current amplitude function $\tilde{C}_+$ for the starting outgoing wave

The derivation of $\tilde{C}_+(l)$ is based on Figures 5 and 6.
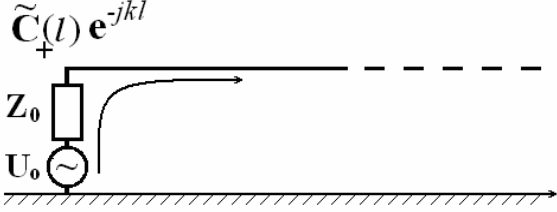

<div style="display:flex"></div>

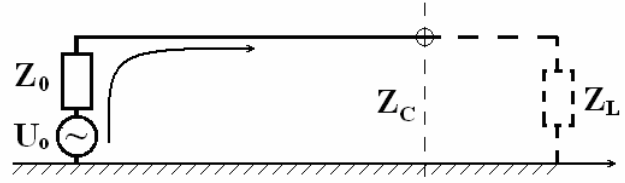Fig. 5: Illustration for the derivation of $\tilde{C}_+(l)$. Fig.6: Fig.6: Infinity formally is "replaced" by Z_C

An infinite wire with a left-hand riser is fed by a voltage source U_0. This means that only an outgoing wave exists, and for the current and for the potential one can make the following equations:

$$i(l) = \tilde{C}_+ e^{-jkl} \quad \text{and} \quad \varphi(l) = Z_C \tilde{C}_+ e^{-jkl} \tag{40a,b}$$

The assumption of an infinite line is made to eliminate reflections from the right hand-side. However, reflections also do not occur at the end, even if the conductor is terminated by Z_C (see Fig. 6). Therefore, the characteristic impedance occurs in the expression for the potential. Taking the sum of (40a, b) one obtains for $\tilde{C}_+(l)$, the analogue result to (33b), namely the amplitude function of the outgoing wave.

$$\tilde{C}_+ = \frac{i(l)Z_C + \varphi(l)}{2Z_C} e^{jkl} \tag{41}$$

Next, the result of (41) is represented with the aid of the matrizant and its elements. It applies:

$$\begin{pmatrix} \varphi(l) \\ i(l) \end{pmatrix} = M(l,0) \begin{pmatrix} U_0 - Z_0 i(0) \\ i(0) \end{pmatrix}, \tag{42}$$

or in terms of the matrizant elements:

$$\varphi(l) = i(l)Z_C = M_{11}(l,0)\big(U_0 - Z_0 i(0)\big) + M_{12}(l,0)i(0) \tag{43}$$

$$i(l) = M_{21}(l,0)\big(U_0 - Z_0 i(0)\big) + M_{22}(l,0)i(0) \tag{44}$$

Division of (43) through (44) yields Z_C:

$$Z_C = \frac{M_{11}(l,0)U_0 + \big(-Z_0 M_{11}(l,0) + M_{12}(l,0)\big)i(0)}{M_{21}(l,0)U_0 + \big(-Z_0 M_{21}(l,0) + M_{22}(l,0)\big)i(0)} \tag{45}$$

Equation (45) now can be resolved with respect to $i(0)$

$$i(0) = \frac{U_0 \big[M_{21}(l,0)Z_C - M_{11}(l,0) \big]}{Z_0 Z_C M_{21}(l,0) - M_{22}(l,0)Z_C - M_{11}(l,0)Z_0 + M_{12}(l,0)} \tag{46}$$

This $i(0)$ is inserted in equations (43) and (44), and then the resulting terms are used in (41). If one still takes into account that the determinant of the matrizant is 1, then one finally arrives at the desired result for $\tilde{C}_+(l)$:

$$\tilde{C}_+(l) = \frac{U_0 e^{jkl}}{-Z_0 Z_C M_{21}(l,0) + M_{22}(l,0) Z_C + M_{11}(l,0) Z_0 - M_{12}(l,0)} \qquad (47).$$

$\tilde{C}_+(l)$ approaches the classical value if one inserts the matrizant elements of (27a) into (47). With this amplitude function for the current one obtains an important intermediate result.

6. Intermediate Result for the current of a horizontal line with two risers

At this stage the development of the formulae $\tilde{R}_+(l), \tilde{R}_-(l)$, and $\tilde{C}_+(l)$ it is possible to describe the current distribution along the line depicted in Fig.2. This is a conductor with two risers and a relatively long horizontal section. In a later step, such a line becomes more complicated by adding an additional scatterer in the central part of the line.

To derive the current on the line, one starts at the left end with the outgoing wave $\tilde{C}_+(l)e^{-jkl}$. This wave is reflected at the right end and runs back to the left: $\tilde{C}_+(l)e^{-jkL}\tilde{R}_-e^{-jk(L-l)}$. At the beginning it is reflected the first time and again runs to the other side: $\tilde{C}_+(l)e^{-jkL}\tilde{R}_-e^{-jkL}\tilde{R}_+e^{-jkl}$. This process repeats itself infinitely often and can be summarized in two sums (see Fig. 7).
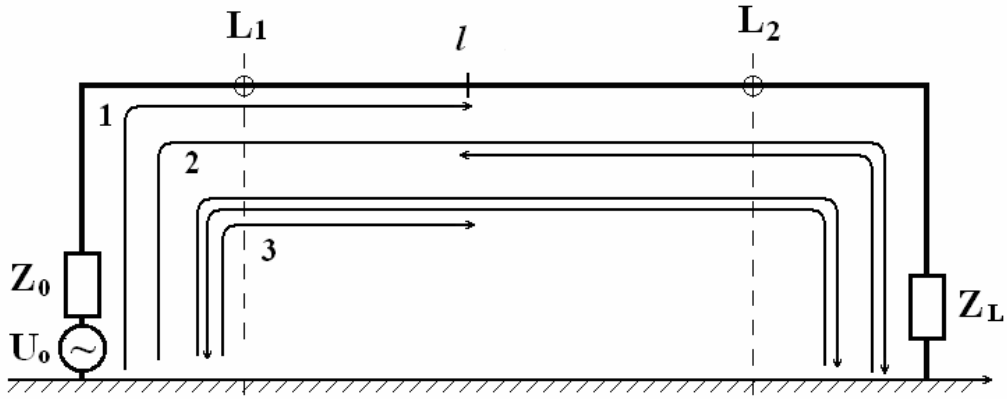

Fig.7: Schematic representation of summing up the first three summands.

$$i(l) = \tilde{C}_+(l) \sum_{n=0}^{\infty} \left(e^{-jkL}\tilde{R}_-e^{-jkL}\tilde{R}_+\right)^n e^{-jkl} + \tilde{C}_+(l)e^{-jkL}\tilde{R}_- \sum_{n=0}^{\infty} \left(e^{-jkL}\tilde{R}_+e^{-jkL}\tilde{R}_-\right)^n e^{-jk(L-l)} \qquad (48)$$

or shorter:

$$i(l) = \frac{\tilde{C}_+(l)\left(e^{-jkl} + \tilde{R}_-e^{-2jkL+jkl}\right)}{1 - \tilde{R}_-\tilde{R}_+e^{-2jkL}} \qquad (49)$$

This is an interesting intermediate result. First, it has its pendant in cTLT with Equation (33a). However, (49) has a much wider validity region: It is not only valid if $kh \ll 1$ (classical theory) but also if $kh \sim 1$. Thus, at these high frequencies of 1-4GHz, the risers at the ends can already be "recognized" (resolved), unlike in the cTLT where the height of the conductor above ground

does not occur in (33a). Another remark to be made here concerns the definition regimes of the functions in (49). The total matrizant solution is divided into three separate parts, which are also solved separately and then later properly matched up again to derive the total solution. Thus, the quantities are defined in the following intervals: $\tilde{C}_+(l)$ in $(L_1 \leq l \leq L_2)$, $\tilde{R}_+(l)$ in $0 \leq l \leq L_2$, and $\tilde{R}_-(l)$ in $L_1 \leq l \leq L$. It should be noted that there is a common interval in which all three functions are defined and become constant: $L_1 \leq l \leq L_2$. In this interval one observes a dominating propagating TEM mode. Therefore, it can be concluded that (49) is only defined in $L_1 \leq l \leq L_2$. However, there is another point of view from which the problem can be considered. Since the matrizant is known for the whole solution along the line, the local coordinate is not restricted to certain intervals in the above formulae containing the matrix elements of the matrizant. All quantities which enter (49) are defined over the total interval $0 \leq l \leq L$. Both perspectives must, however, guarantee that the TEM modes dominate in the vicinity of the ends of the line. Between these two TEM-pieces the line may become again inhomogeneous. This will become the subject of the next chapters.

IV. TRANSMISSION AND REFLECTION COEFFICIENTS OF THE SCATTERER

At this stage of the work the wiring is changed so that a scatterer is inserted in the central area of the line. The situation is shown in Fig. 8.
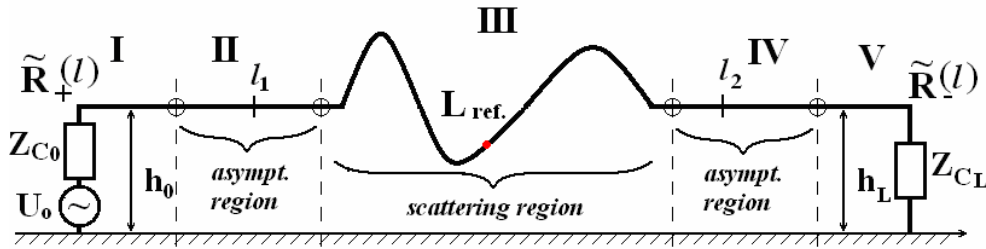

Fig. 8: Schematic representation of a conductor with two risers, two parallel sections, and a scatterer in the central part.

In Fig.8 the line is composed of five parts: The scatterer in the middle part (part **III**) is embedded in two asymptotic regions (parts **II** and **IV**), each of which make connections to the risers (parts **I** and **V**). The two parallel parts of the line may have different heights above ground. At an appropriate point inside the scatterer a reference point $L_{ref.}$ is selected. If the scatterer represents a horizontal bend, then the reference point could be exactly at the bend point.

Now, there are again two ways to calculate the current distribution along such a conductor. First, one can calculate all five parts of the line individually. When assembling the individual solutions one must, however, ensure that the line parameters are matched against each other at the joints. Or, one calculates the matrizant for the entire line and then splits it into several parts according to

$$M(L,0) = M(L,L_4) \cdot M(L_4,L_3) \cdot M(L_3,L_2) \cdot M(L_2,L_1) \cdot M(L_1,0) \qquad (50)$$

In the second case one already has all five partial solutions available and they can be used to calculate all reflection- and transmission coefficients of the line. This takes place in several steps.

In step one it is assumed that a wave coming from the left is approaching the scatterer whereby one portion $\tilde{D}_{0+}$ of the wave is passing the scatterer and another portion $\tilde{R}_{0+}$ is reflected by the scatterer. The configuration is depicted in Fig.9.
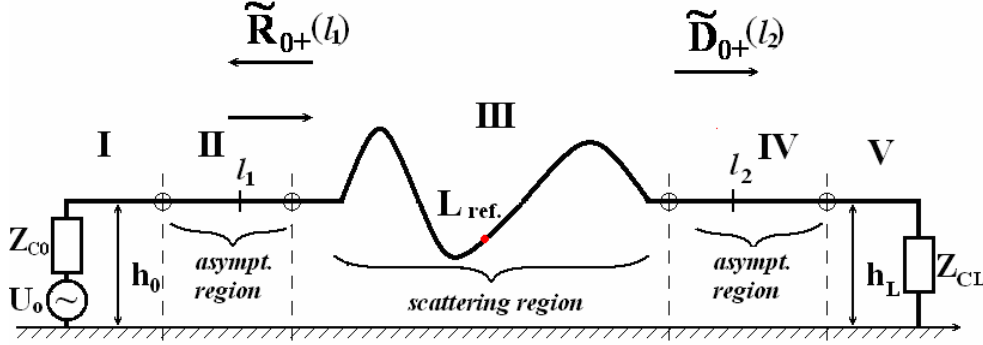

Fig. 9: Representation for the calculation of $\tilde{R}_{0+}$ and $\tilde{D}_{0+}$.

Choosing a $l_1 \in \mathbf{II}$, the TEM region, then one obtains the usual equations:

$$i(l_1) = \tilde{I}_0 \left(e^{-jk(l_1 - L_{ref})} + \tilde{R}_{0+} e^{jk(l_1 - L_{ref})} \right) \quad \text{and} \quad \varphi(l_1) = \tilde{I}_0 Z_{C_0} \left(e^{-jk(l_1 - L_{ref})} - \tilde{R}_{0+} e^{jk(l_1 - L_{ref})} \right) \quad (51a,b)$$

Solving for $\tilde{R}_{0+}$ gives

$$\tilde{R}_{0+}(l_1) = e^{-2jk(l_1 - L_{ref})} \frac{i(l_1) Z_{C_0} - \varphi(l_1)}{i(l_1) Z_{C_0} + \varphi(l_1)} \quad (52)$$

Note that the zero phases always occur at the locations of the reference points of the scatterers.

For the transmission coefficient, the following equations are valid in zone $\mathbf{IV}$.

$$i(l_2) = \tilde{I}_0 e^{-jk(l_2 - L_{ref})} \tilde{D}_{0+} \quad \text{and} \quad \varphi(l_2) = \tilde{I}_0 Z_{C_L} e^{-jk(l_2 - L_{ref})} \tilde{D}_{0+} \quad (53a,b)$$

On the other hand, one has the relation:

$$\begin{pmatrix} \varphi(l_1) \\ i(l_1) \end{pmatrix} = M(l_1, l_2) \begin{pmatrix} \varphi(l_2) \\ i(l_2) \end{pmatrix} \quad (54)$$

Equations (51a, b) are inserted into the left hand side of (54), while one uses (50a, b) together with the known Matrizant in the right hand side of (54). Then, one arrives at two equations for $\tilde{R}_{0+}$ and $\tilde{D}_{0+}$, and afterwards can solve them, which results in:

$$\tilde{D}_{0+}(l_2) = \frac{2 Z_{C_0} e^{jk(l_2 - l_1)}}{M_{11}(l_1, l_2) Z_{C_L} + M_{12}(l_1, l_2) + M_{21}(l_1, l_2) Z_{C_0} Z_{C_L} + M_{22}(l_1, l_2) Z_{C_0}} \quad (55)$$

and

$$\tilde{R}_{0+}(l_1) = e^{-2jk(l_1 - L_{ref})} \frac{\left[-M_{11}(l_1, l_2) Z_{C_L} - M_{12}(l_1, l_2) + M_{21}(l_1, l_2) Z_{C_0} Z_{C_L} + M_{22}(l_1, l_2) Z_{C_0} \right]}{\left[M_{11}(l_1, l_2) Z_{C_L} + M_{12}(l_1, l_2) + M_{21}(l_1, l_2) Z_{C_0} Z_{C_L} + M_{22}(l_1, l_2) Z_{C_0} \right]} \quad (56)$$

In step two a wave coming from the right is considered which is partially reflected ($\tilde{R}_{0-}$) and partially transmitted ($\tilde{D}_{0-}$) by the scatterer. Figure 10 sketches this situation.
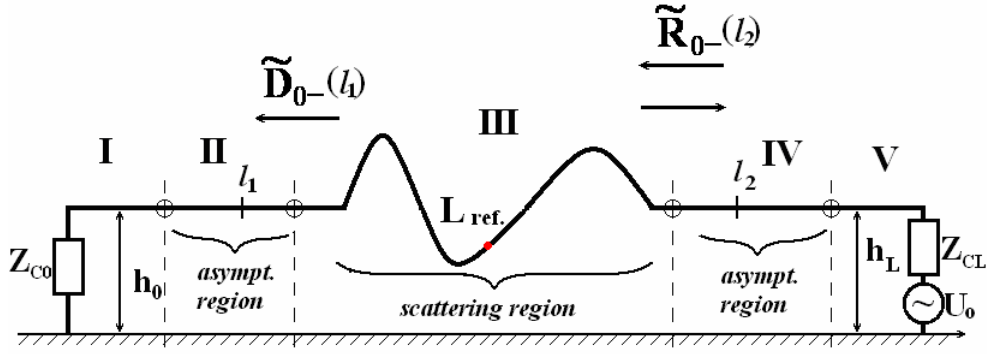
Fig. 10: Sketch for the estimation of $\tilde{D}_{0-}$ and $\tilde{R}_{0-}$.

Analogous to equations (51) and (53) one now starts with two similar equations:

$$\varphi(l_1) = -\tilde{I}_0 \tilde{D}_{0-} Z_{C_0} e^{jk(l_1 - L_{ref})} \qquad \text{and} \qquad i(l_1) = \tilde{I}_0 \tilde{D}_{0-} e^{jk(l_1 - L_{ref})} \qquad (57a,b)$$

and

$$\varphi(l_2) = \tilde{I}_0 Z_{C_L} \left[-e^{jk(l_2 - L_{ref})} + \tilde{R}_{0-} e^{-jk(l_2 - L_{ref})} \right], \quad i(l_2) = \tilde{I}_0 \left[e^{jk(l_2 - L_{ref})} + \tilde{R}_{0-} e^{-jk(l_2 - L_{ref})} \right] \quad (58a,b)$$

The right hand sides of (57) and (58) are inserted in the matrizant relation (59)

$$\begin{pmatrix} \varphi(l_2) \\ i(l_2) \end{pmatrix} = M(l_2, l_1) \begin{pmatrix} \varphi(l_1) \\ i(l_1) \end{pmatrix} \qquad (59)$$

This again leads to two equations for the two unknowns $\tilde{R}_{0-}$ and $\tilde{D}_{0-}$.

$$\tilde{D}_{0-}(l_1) = \frac{2 Z_{C_L} e^{jk(l_2 - l_1)}}{M_{11}(l_2,l_1) Z_{C_0} - M_{12}(l_2,l_1) - M_{21}(l_2,l_1) Z_{C_0} Z_{C_L} + M_{22}(l_2,l_1) Z_{C_L}} \qquad (60)$$

$$\tilde{R}_{0-}(l_2) = e^{2jk(l_2 - L_{ref})} \frac{\left[-M_{11}(l_2,l_1) Z_{C_0} + M_{12}(l_2,l_1) - M_{21}(l_2,l_1) Z_{C_0} Z_{C_L} + M_{22}(l_2,l_1) Z_{C_L} \right]}{\left[M_{11}(l_2,l_1) Z_{C_0} - M_{12}(l_2,l_1) - M_{21}(l_2,l_1) Z_{C_0} Z_{C_L} + M_{22}(l_2,l_1) Z_{C_L} \right]} \qquad (61)$$

Based on the results of (55), (56), and (60), (61) *the third step* can be carried out: namely, the estimation of the current in the interval $\left[0, L_{ref} \right]$.

By introducing a further reflection coefficient $\tilde{R}_{0\Sigma}$ the subsequent calculation can be simplified. Its effect is shown in Figure 11.
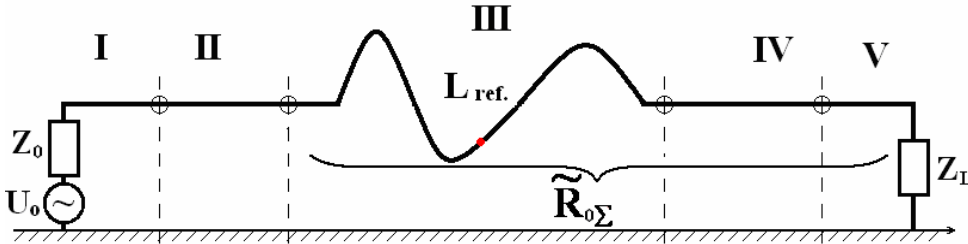

Fig.11: Sketch of the effect of $\tilde{R}_{0\Sigma}$.

In order to express $\tilde{R}_{0\Sigma}$ in relation to all the other reflection and transmission coefficients, $\tilde{R}_{0+}$, $\tilde{D}_{0+}$, $\tilde{R}_{0-}$, $\tilde{D}_{0-}$, and $\tilde{R}_-$, one assumes a wave coming from $-\infty$ that is partially passing through the scatterer ($\tilde{D}_{0+}$) and partially being reflected by the scatterer ($\tilde{R}_{0+}$). At the end of the line it is again reflected ($\tilde{R}_-$) and runs backward, again partially passing through the scatterer ($\tilde{D}_{0-}$) and partially being reflected ($\tilde{R}_{0-}$). All parts of the waves passing through the scatterer coming from the right vanish at $-\infty$. However, the scattering process between the inhomogeneous part of the conductor and the end of the line is repeated an infinite number of times (see Fig.12).
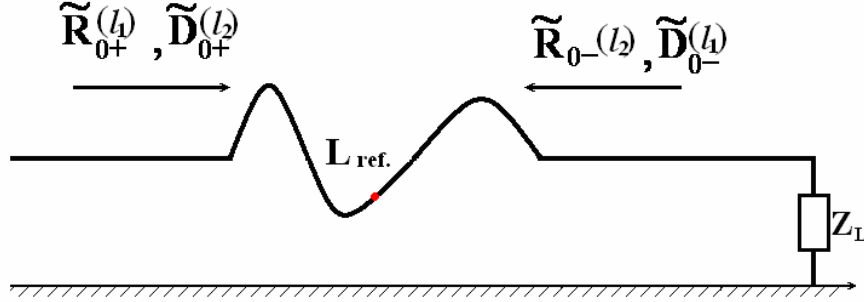

Fig.12: Definition of the reflection coefficient $\tilde{R}_{0\Sigma}$

The distance between L_{ref} (the coordinate origin for this process) and the end of the line L is denoted by $\tilde{L} := L - L_{ref}$. Then, one gets for $\tilde{R}_{0\Sigma}$:

$$\tilde{R}_{0\Sigma} = \tilde{R}_{0+} + \tilde{D}_{0+}e^{-jk\tilde{L}}\tilde{R}_-e^{-jk\tilde{L}}\tilde{D}_{0-} + \tilde{D}_{0+}e^{-jk\tilde{L}}\tilde{R}_- \underbrace{e^{-jk\tilde{L}}\tilde{R}_{0-}e^{-jk\tilde{L}}\tilde{R}_-}_{periodical\ part}\tilde{D}_{0-} + ... \tag{62}$$

or

$$\tilde{R}_{0\Sigma} = \tilde{R}_{0+} + \tilde{D}_{0+}e^{-jk\tilde{L}}\tilde{R}_-\sum_{n=0}^{\infty}\left(e^{-jk\tilde{L}}\tilde{R}_{0-}e^{-jk\tilde{L}}\tilde{R}_-\right)^n e^{-jk\tilde{L}}\tilde{D}_{0-} = \tilde{R}_{0+} + \frac{\tilde{D}_{0+}\tilde{R}_-\tilde{D}_{0-}e^{-2jk\tilde{L}}}{1-\tilde{R}_{0-}\tilde{R}_-e^{-2jk\tilde{L}}} \tag{63}$$

At this point, a result (49) of the previous chapter is used and rewritten on the present reflection coefficient $\tilde{R}_{0\Sigma}$.

$$i^{(1)}(l) = \tilde{C}_+ \frac{e^{-jkl} + \tilde{R}_{0\Sigma}e^{-2jkL_{ref}+jkl}}{1-\tilde{R}_{0\Sigma}\tilde{R}_+e^{-2jkL_{ref}}}, \ l \in \left[0, L_{ref}\right] \tag{64}$$

Replacing $\tilde{R}_{0\Sigma}$ in (64) by expression (63) one obtains a longer equation for $i^{(1)}(l)$:

$$i^{(1)}(l) = \tilde{C}_+\left\{\left[1-\tilde{R}_{0-}\tilde{R}_-e^{-2jk\tilde{L}}\right]e^{-jkl} + \left(\tilde{R}_{0+} + \tilde{R}_-\left(\tilde{D}_{0+}\tilde{D}_{0-} - \tilde{R}_{0+}\tilde{R}_{0-}\right)e^{-2jk\tilde{L}}\right)e^{-2jkL_{ref}+jkl}\right\} \cdot$$
$$\cdot\left\{1-\tilde{R}_{0-}\tilde{R}_-e^{-2jk\tilde{L}} - \tilde{R}_+\tilde{R}_{0+}e^{-2jkL_{ref}} - \tilde{R}_-\tilde{R}_+\left(\tilde{D}_{0+}\tilde{D}_{0-} - \tilde{R}_{0+}\tilde{R}_{0-}\right)e^{-2jkL_{ref}}\right\}^{-1} \tag{65}$$

Finally, *in the last step* the current $i^{(2)}(l)$ for $l \in \left[L_{ref}, L\right]$ remains to be estimated.

An incoming wave from the left $\tilde{I}_0 e^{-jk\tilde{l}}$ ($\tilde{l} := l - L_{ref}$) passes the scatterer and is reflected at the end by $\tilde{R}_-$, runs via $\tilde{l}$ back to the scatterer and there is reflected again. This process is repeated infinitely often (for explanations see Fig.13).
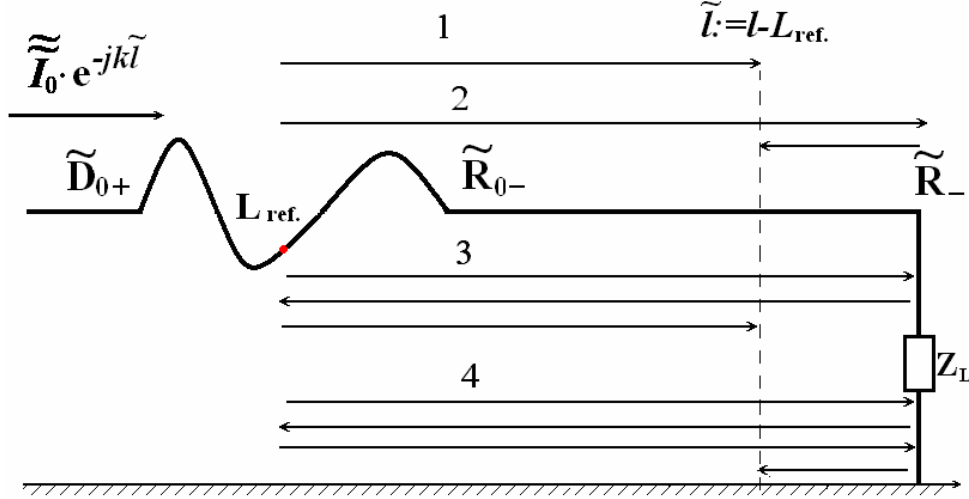
Fig.13: Scattering process between scatterer and the end of the line.

Translating the above scattering process into a formula yields:

$$i^{(2)}(l) = \tilde{\tilde{I}}_0 \left[\tilde{D}_{0+}e^{-jk\tilde{l}} + \tilde{D}_{0+}e^{-jk\tilde{L}}\tilde{R}_-e^{-jk(\tilde{L}-\tilde{l})} + \tilde{D}_{0+}e^{-jk\tilde{L}}\tilde{R}_-e^{-jk\tilde{L}}\tilde{R}_{0-}e^{-jk\tilde{l}} + \tilde{D}_{0+}e^{-jk\tilde{L}}\tilde{R}_-e^{-jk\tilde{L}}\tilde{R}_{0-}e^{-jk\tilde{L}}\tilde{R}_-e^{-jk(\tilde{L}-\tilde{l})} + ... \right] =$$

$$= \tilde{\tilde{I}}_0 \left\{ \frac{\tilde{D}_{0+}e^{-jk\tilde{l}}}{1 - \tilde{R}_-\tilde{R}_{0-}e^{-2jk\tilde{L}}} + \frac{\tilde{D}_{0+}\tilde{R}_-e^{-2jk\tilde{L}+jk\tilde{l}}}{1 - \tilde{R}_-\tilde{R}_{0-}e^{-2jk\tilde{L}}} \right\} = \tilde{\tilde{I}}_0\tilde{D}_{0+} \frac{e^{-jk(l-L_{ref})} + \tilde{R}_-e^{-2jk\tilde{L}+jk(l-L_{ref})}}{1 - \tilde{R}_-\tilde{R}_{0-}e^{-2jk\tilde{L}}}$$

(66)

In (66) all quantities are known except the amplitude function $\tilde{\tilde{I}}_0(l)$. This function is taken from the outgoing wave part from (64):

$$\tilde{\tilde{I}}_0(l) = \frac{\tilde{C}_+(l)e^{-jkL_{ref}}}{1 - \tilde{R}_{0\Sigma}\tilde{R}_+e^{-2jkL_{ref}}}$$

(67)

Equation (67) is now used in (66), $\tilde{R}_{0\Sigma}$ is replaced by (63), and finally one obtains the result for $i^{(2)}(l)$:

$$i^{(2)}(l) = \frac{\tilde{C}_+\tilde{D}_{0+}\left[e^{-jkl} + \tilde{R}_-e^{-2jk(L_{ref}+\tilde{L})+jkl} \right]}{1 - \tilde{R}_{0-}\tilde{R}_-e^{-2jk\tilde{L}} - \tilde{R}_+\tilde{R}_{0+}e^{-2jkL_{ref}} - \tilde{R}_-\tilde{R}_+\left(\tilde{D}_{0+}\tilde{D}_{0-} - \tilde{R}_{0+}\tilde{R}_{0-} \right)\cdot e^{-2jk(L_{ref}+\tilde{L})}}, \quad l \in \left[L_{ref}, L \right]$$

(68)

With (64) and (68), the current distribution along the entire line is known, expressed in terms of reflection and transmission coefficients. The quantity $\tilde{C}_+$ is taken from the previous chapter, as well as the quantities $\tilde{R}_+(l)$ and $\tilde{R}_-(l)$.

A special case of the above general scatterer would be a horizontal line conducted horizontally above ground with a bend. In this case, some formulae can be simplified according to $\tilde{R}_{0-} = \tilde{R}_{0+} \equiv \tilde{R}_0$, $\tilde{D}_{0+} = \tilde{D}_{0-} \equiv \tilde{D}_0$, and $Z_{C_0} = Z_{C_L}$.

V. NUMERICAL EXAMPLES AND DISCUSSION

Recently, a numerical example was shown [17] for a uniform TL above a conducting ground plane with risers on each end. The horizontal length of the line was 200 cm and the height over ground was 5 cm leading to a total arc length of 210 cm for the TL. It could be shown that the matrizant of the whole line can be composed of the matrizants for the riser regions (using TLST) and the classical matrizant for the asymptotical uniform part between the riser regions. It was also shown that the current in the asymptotical region can be calculated using the concept of advanced reflection coefficients $\tilde{R}_+$ and $\tilde{R}_-$ which can be calculated using the parameter matrix elements of the TLST analysis of the riser regions. In the following section, non-uniformity is also allowed in the middle region of the TL. This non-uniformity can be local, as for example a single bend in the line, or there can be a region with distributed non-uniformity.

1.   Horizontal line with one bend

First, a single local bend in the middle of an otherwise uniform TL with risers on each end is investigated. The TL configuration is shown in Fig. 14.
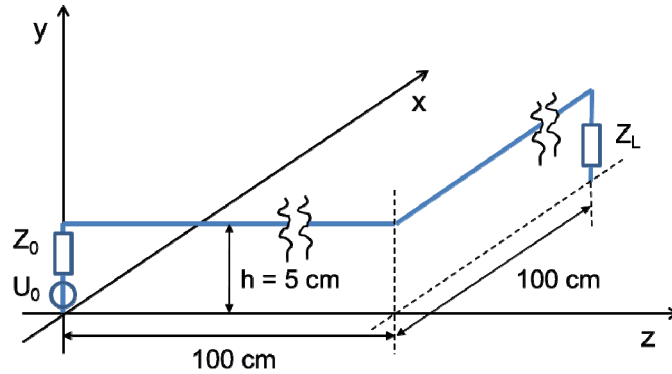

Fig. 14: Uniform TL with risers at each end and a 90° bend in the middle of the TL.

The height of the risers is $h = 5$ cm. The length of the horizontal part between the risers is 200 cm and there is a 90° bend exactly in the middle of the line. In TLST the natural parameter of the TL is the arc length l. The top of the left riser is at $l = 5$ cm, the horizontal bend at $l = 105$ cm, the top of the right riser at $l = 205$ cm and the end of the line at $l = 210$ cm. This leads to a total TL arc length of $L = 210$ cm. The position of the horizontal bend is designated by $L_{ref} = 105$ cm. On the left side the TL is driven by voltage source with $U_0 = 1$ V and source impedance $Z_0 = 50$ Ω. The line is terminated with load impedance $Z_L = 50$ Ω at the right end.

For the TL configuration of Fig.14 a TLST analysis [8] was performed leading to the local, frequency dependent and complex valued TL parameter matrix elements shown in Fig. 15.
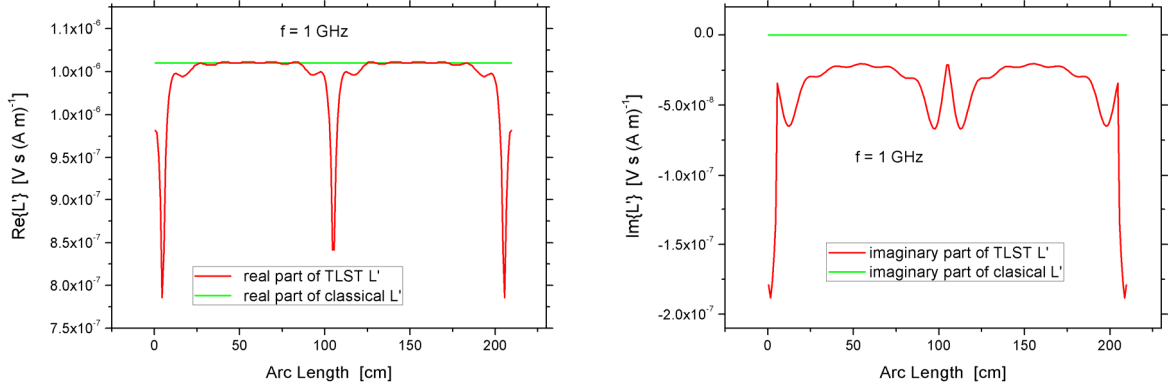
Fig. 15 :   TLST parameter matrix elements for the TL with risers and 90° bend from Fig. 14 at a frequency of 1 GHz corresponding to the per unit length inductance of a classical TL.

Regarding the real part of the TLST parameter matrix element $P^{*(1)}_{12}$ – corresponding to the per unit length inductance L' of a classical TL – the deviations from the classical value in the riser regions and at the 90° bend in the middle of the TL are obvious (Fig. 15 left). But there are two regions between the risers and the middle bend were the classical L' values are reached and, therefore, the TEM mode is dominant. This is true for the arc length region from about $l = 22$ cm to $l = 88$ cm and $l = 122$ cm to $l = 188$ cm. In Fig. 15 (right) the imaginary part of the L' correspondence is shown to be zero for the classical TL, because in classical transmission-line theory radiation effects do not occur. In TLST radiation effects are included and, therefore, the parameter matrix elements are complex in general. Although radiation is a cooperative process of the whole TL [7], the troughs at the riser positions and at the horizontal bend indicate the most radiating parts of the TL where there is a distinct non-uniformity of the line. The matrizants introduced in section II are calculated using the elements of the TLST parameter matrix $\mathbf{P}^{*(1)}$ [8].

For further investigation of the TL model (Fig. 14) the arc lengths l_1 and l_2 are set in the respective asymptotic regions using $l_1 = 55$ cm and $l_2 = 155$ cm. According to the formulas in section III.2 the reflection coefficients $\tilde{R}_-(l_2)$ and $\tilde{R}_+(l_1)$ for the line ends are calculated where $\tilde{R} \equiv \tilde{R}_-(l_2) = \tilde{R}_+(l_1)$ because of symmetry. For the local scatterer (horizontal 90° bend in the middle of the TL) at arc length $l = L_{\text{ref}} = 105$ cm (reference point) the reflection and transmission coefficients were calculated according to the formulas in section III. Because of the symmetry of the TL in relation to the reference point, one can write $\tilde{R}_0 \equiv \tilde{R}_{0-}(l_2) = \tilde{R}_{0+}(l_1)$ and $\tilde{D}_0 \equiv \tilde{D}_{0+}(l_2) = \tilde{D}_{0-}(l_1)$. Fig.16 shows the frequency dependency of the mentioned coefficients. Both terminating impedances on the left and right end of the TL have a value of 50 Ω resulting in a constant classical reflection coefficient $R_{\text{class}} = 0.73$. Because of radiation effects and the generation of non TEM modes in the non-uniform, bent TL, the TLST reflection coefficient $|\tilde{R}|$ decreases from the classical value at higher frequencies.
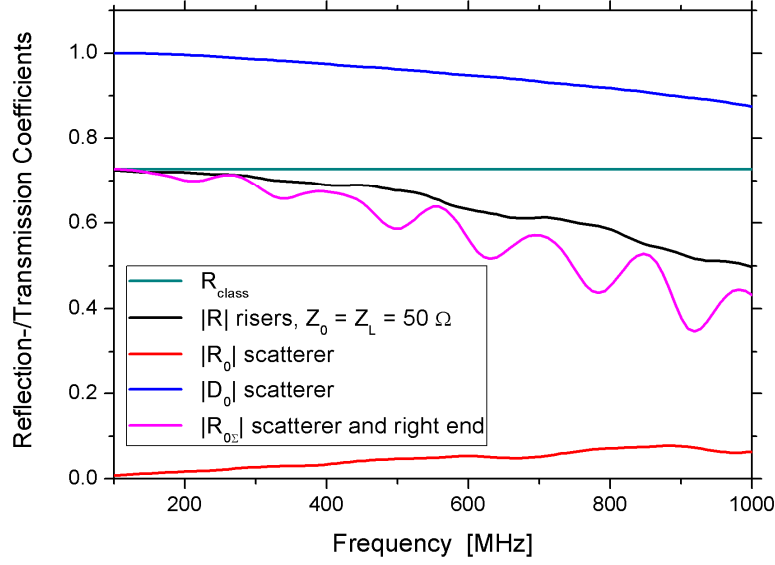
21

Fig. 16:   Advanced and frequency dependent reflection and transmission coefficients for the TL with risers at the ends and a local bend in the middle of the line.

The TLST transmission coefficient $|\tilde{D}_0|$ for the local scatterer is 1 for low frequencies and decreases also for higher frequencies. The corresponding reflection coefficient $|\tilde{R}_0|$ is 0 for low frequencies and increases for higher frequencies because of the mentioned radiating energy losses and the generation of non TEM modes, mainly in the vicinity of the non-uniform parts of the TL. The reflection coefficient $\tilde{R}_{0\Sigma}$ is a kind of combination of the right hand reflection coefficient $\tilde{R}_-$ for the termination of the line (including the riser effects) and the transmission and reflection coefficients of the local scatterer $\tilde{D}_0$ and $\tilde{R}_0$.
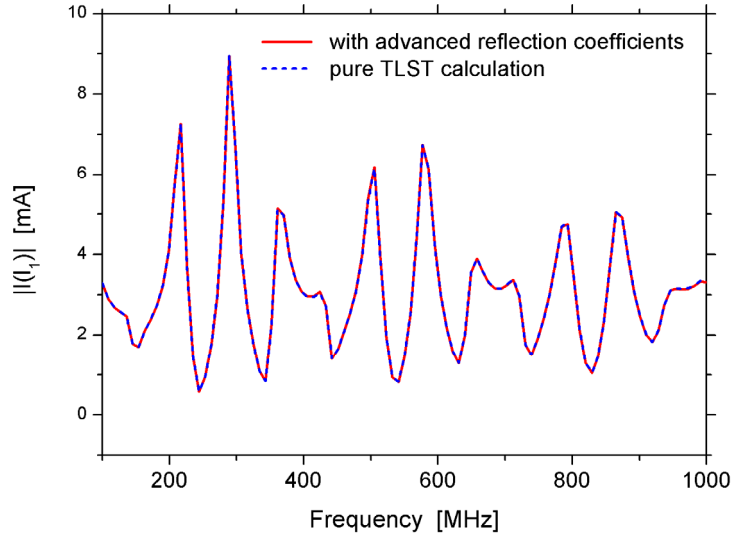

Fig. 17:   Current in the left hand asymptotic region at position l_1 of the TL configuration according to Fig.14.

Part of the initial electromagnetic wave coming from the voltage source on the left side of the TL bounces back and forth between the scattering center at the right hand riser and the local scatterer (90° bend) in the middle of the TL. This is the reason for the oscillation in the course of $\left| \tilde{R}_{0\Sigma} \right|$.

Using formula (64) for the current in the left hand asymptotic region at l_1 it can be shown that there is an excellent agreement with the current resulting from a pure TLST calculation. This situation is shown above in Fig. 17.

The correspondence for the current in the right hand asymptotic region at position l_2 (according to formula (68)) with the pure TLST calculation is also excellent. The frequency dependent course of $|I(l_2)|$ is shown in Fig. 18.
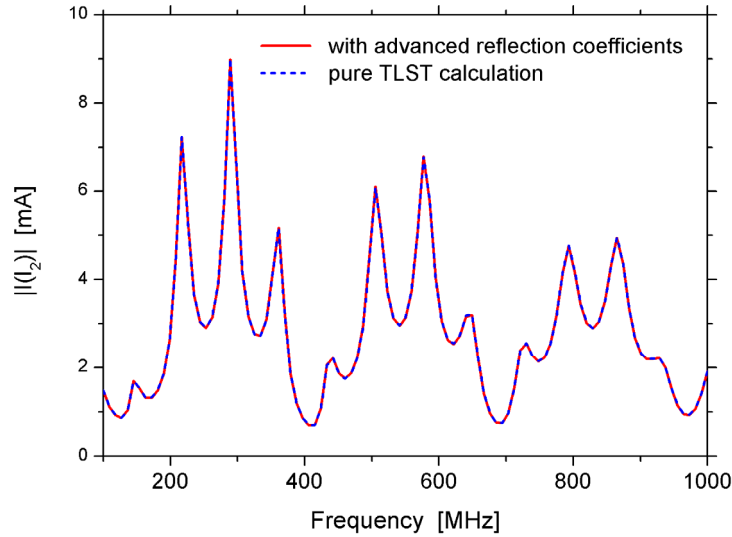

Fig. 18:   Current in the right hand asymptotic region at position l_2 of the TL configuration, according to Fig.14.

2. *Simple one line simulator*

Now, the local non-uniformity in the middle of the TL is replaced by a distributed non-uniformity. The course of the TL is defined so that there is still a left and right hand asymptotical region between the left and right hand risers and the distributed non-uniformity is in the middle part. The actual geometry is displayed in Fig. 19. One can think of a projection of an open TEM waveguide structure onto the vertical axial plane (yz-plane). The total dimension of the TL in z-direction is again 2 m. Because of the risers and the distinct vertical extent, the total arc length with $L = 252.5$ cm is significantly larger. Starting with arc length $l = 60$ cm there is a slope up to the top bend which is also defined as the reference point with $L_{ref} = 144$ cm. From the top bend there is a relatively steep decline towards the right hand asymptotical region, which again is at a height of 5 cm above the conducting ground plane.

Fig. 20 shows the L' like real part of the $P^{*(1)}_{12}$ parameter matrix element of TLST analysis along the TL arc length for a frequency of $f = 1$ GHz. It is obvious that there is significant deviation from the classical constant value. The bends of two risers, i.e., the top bend and the bend between the right-hand end of the distributed non-uniform region and the right-hand asymptotical region, lead to distinct troughs in the real part of L'. In the left slope region there is little oscillation, while in the steeper right hand slope region oscillation is obvious, which shows the presence of leaky modes [18]. It is also obvious that actual TL values (real part of L') in the asymptotical regions do not fit to the classical values as well as in the previous example (see Fig.15). The reason for this is that the assumptions for an asymptotical region are not fulfilled very well because of the shortness of the horizontal TL parts. But, later on, it is shown that even with these restricted conditions the current in the asymptotical regions can be calculated quite accurately.
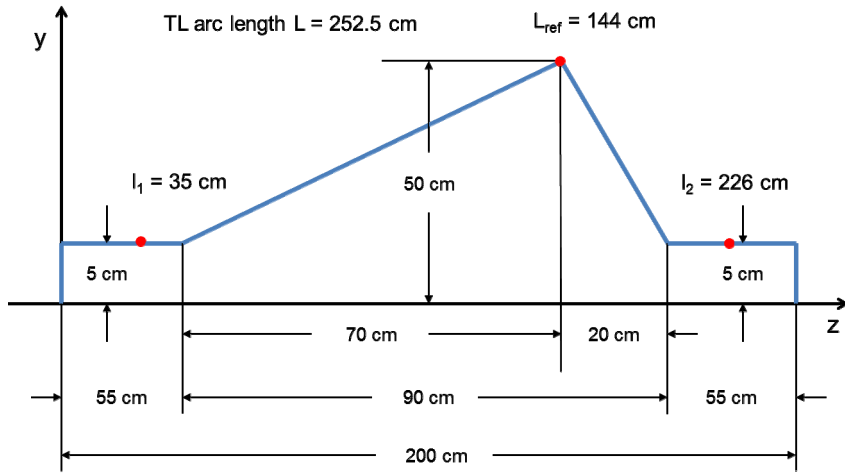
Fig. 19: Construction details of the TL with left and right hand risers and a vertically distributed non-uniformity in the middle part.
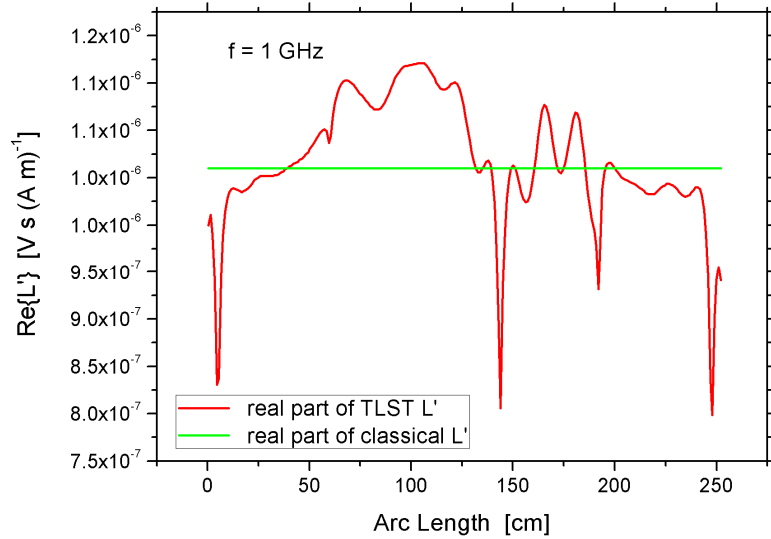

Fig. 20: Real part of *L'* like TLST parameter matrix element for the TL with risers and distributed non-uniformity in the middle part, according to Fig.19.

The appropriate reflection coefficients for the riser parts and the reflection and transmission coefficients for the distributed non-uniform middle part were calculated according to the formulas in the previous sections using the TLST matrizants for the actual TL configuration from Fig.19. The results are shown in Fig. 21. Of course, now the values for $\tilde{R}_{0+}$ and $\tilde{R}_{0-}$ differ because there is no longer any symmetry for the TL model. However, it can be generally shown from (55) and (60) that $\tilde{D}_{0-}$ and $\tilde{D}_{0+}$ are always equal to each other. If this does not result from the numerics then the asymptotic regions around the scatterers were not chosen large enough. In order to not overload Figure 21 only the "+" values are shown.
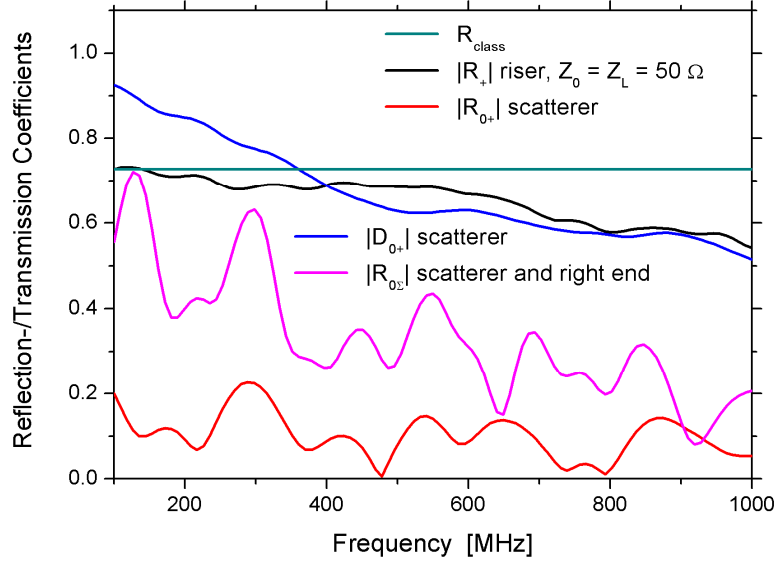
Fig. 21: Advanced and frequency dependent reflection and transmission coefficients for the TL with risers and distributed non-uniformity in the middle of the line (simple one line simulator)

Because of the stronger non-uniformity of the middle part in the actual TL model, the transmission coefficient $\tilde{D}_{0+}$ is significantly smaller and the reflection coefficient $\tilde{R}_{0+}$ significantly larger than in the previous example, while reflection coefficients for the line ends remain nearly the same. The shown coefficients of Fig. 21 were calculated for arc length $l_1 = 35$ cm, which is in the left hand asymptotic region (see Fig 19). The "-"coefficients needed for the further current calculations were calculated for arc length $l_2 = 226$ cm lying in the right hand asymptotic region.
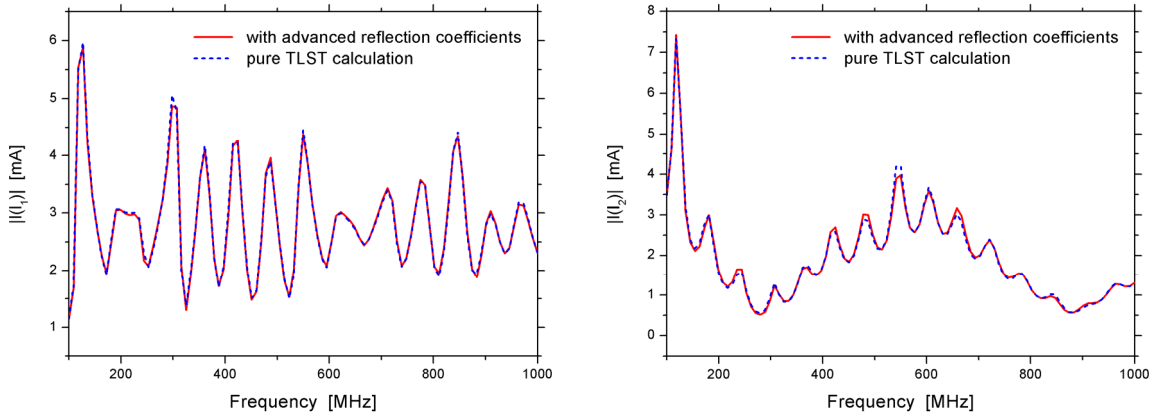

Fig. 22: Currents (magnitude) in the asymptotical regions at l_1 (left) and l_2 (right) using advanced reflection and transmission coefficients in comparison with pure TLST calculations.

Using the appropriate calculated coefficients for the current determination according to (64) and (68) it can be shown that the agreement with pure TLST calculations is again very good. The results are shown in Fig. 22 for the current at arc lengths $l = l_1$ (left) and $l = l_2$ (right). Although the requirements for an asymptotic region are not perfectly fulfilled, as discussed above, the developed evaluation procedure seems to be quite tolerant of this fact.

VI. CONCLUSION

In the TLST, the derived generalized reflection and transmission coefficients in this paper are used to calculate the currents along practical layouts of non-homogeneous transmission lines. The obtained results were compared with those of an exact TLST calculation, and an excellent agreement was observed in the investigated high frequency region. Note, that for the derivation of the $R's$ and $D_0's$, parallel conductor sections with dominating TEM modes were necessary between the central scatterer and the non-homogeneous risers. Thus, radiation interaction was restricted only within the individual inhomogeneous conductor parts. Even an extension in the higher GHz realm (up to 4 GHz) did not change the excellent agreement of the results for the currents. The representation of the currents in terms of local and frequency dependent reflection and transmission coefficients lead to formulas which resemble those of classical TL theory. In particular, the formulas are quite practical when solving for current poles in the complex plane, and thus facilitate an SEM analysis [19].

REFERENCES

1. H. Haase and J. Nitsch, "Full-wave transmission line theory (FWTLT) for the analysis of three-dimensional wire-like structures," *in Proceedings of 14th International Zurich Symposium on EMC,* Feb. 2001, pp. 235-240.
2. H. Haase, J. Nitsch, and T. Steinmetz, „Transmission - Line Super Theory: A New Approach to an Effective Calculation of Electromagnetic Interactions", *Radio Science Bulletin,* 307, 2003, pp. 33-60.
3. H. Haase, T. Steinmetz, and J. Nitsch, "New Propagation Models for Electromagnetic Waves along Uniform and Non-uniform Cables," *IEEE Transaction on Electromagnetic Compatibility,* EMC-47, 3, 2004, pp. 345-352.
4. J. Nitsch and S. Tkachenko, "Newest Developments in Transmission - Line Theory and Applications", *Interaction Notes*, Note 592.
5. J. Nitsch and S. Tkachenko, "Global and Modal Parameters in the Generalized Transmission Line Theory and their Physical Meaning"; *Radio Science Bulletin,* 312,March 2005, pp.21-31.
6. J. Nitsch, S. Tkachenko, „High-frequency Multiconductor Transmission line Theory", *Foundation of Physics* (2010) 40: 1231-1252, DOI 10.1007/s10701-010-9443-1.
7. J. Nitsch, G. Wollenberg, and F. Gronwald, *Radiating Nonuniform Transmission-Line Systems and the Partial Element Equivalent Circuit Method*, Wiley 2009.
8. R. Rambousky, J. B. Nitsch, and H. Garbe, "Application of the Transmission-Line Super Theory to Multi-wire TEM-Waveguide Structures", *IEEE Transaction on Electromagnetic Compatibility,* EMC-55, 6, 2013, pp. 1311-1319.
9. S. Tkachenko, F. Rachidi, and M. Ianoz, "High-frequency electromagnetic field coupling to long terminated lines", *IEEE Transactions on Electromagnetic Compatibility*, Vol. 43, No. 2, May 2001, p.117-129.
10. F. Rachidi and S. Tkachenko, eds., *Electromagnetic Field Interaction with Transmission Lines: From Classical Theory to HF Radiation Effects*" (Chapters 4 and 5), WIT Press 2008
11. S.V. Tkachenko, J. Nitsch, R. Vick, F. Rachidi, D. Poljak, "Singularity expansion method (SEM) for long terminated transmission lines", 2013 International Conference on Electromagnetics in Advanced Applications (ICEAA), Torino, 9-13 Sept. 2013, pp: 1091 – 1094.
12. S.Tkachenko, F. Rachidi, M. Ianoz, "Electromagnetic Field Coupling to a Line of Finite Length: Theory and a Fast Iterative Solutions in Frequency and Time domains," *IEEE Transaction on Electromagnetic Compatibility,* vol. 37, No. 4, November 1995.

13. S. Tkachenko, F. Middelstaedt; J. Nitsch, R. Vick, G. Lugrin, F. Rachidi, "High-frequency electromagnetic field coupling to a long finite line with vertical risers", In the Transaction, *Proceedings of the General Assembly of the International Union of Radio Sciences (URSI)*, Beijing, 2014 (DOI: 10.1109/URSIGASS.2014.6929526).

14. K. K. Mei, "Theory of Maxwellian Circuits", *Rad. Sci. Bul.*, 305, 2003, pp.6-13.

15. F. R. Gantmacher, The Theory of Matrices, vol.2, Chelsea, New York (1984).

16. H. Haase, J.Nitsch, S. Tkachenko, "A Full-Wave Transmission Line Theory", 2005 International Conference on Electromagnetics in Advanced Applications (ICEAA), Torino, Italy, Sept. 2005.

17. R. Rambousky, J. Nitsch, and S. Tkachenko, "Application of Transmission – Line Super Theory to Classical Transmission Lines with Risers", submitted for publication in Adv. Rad. Sci., Sept. 2014.

18. J. Nitsch, S. Tkachenko, "Physical Interpretation of the Parameters in the Full-Wave Transmission-Line Theory", ISTET 2009, XV International Symposium on Theoretical Electrical Engineering, Lübeck, 22-24 June, Germany.

19. F. Mittelstädt, S. Tkachenko, R. Vick, and R. Rambousky, „Analytic Approximation of Natural Frequencies of Bent Wire Structures above Ground", submitted for publication to the joined International IEEE Symposium and EMC EUROPE 2015, Dresden, Germany.